Network of Remote and Local Protein Dynamics in Dihydrofolate Reductase Catalysis

ARTICLE *in* ACS CATALYSIS · APRIL 2015

Impact Factor: 9.31 · DOI: 10.1021/acscatal.5b00331

1 AUTHOR:

Priyanka Singh

University of Iowa

6 PUBLICATIONS **33** CITATIONS

ACS Catalysis

Research Article

pubs.acs.org/acscatalysis

Network of Remote and Local Protein Dynamics in Dihydrofolate Reductase Catalysis

Priyanka Singh, Kevin Francis, and Amnon Kohen*

The Department of Chemistry, The University of Iowa, Iowa City, Iowa 52242, United States

Supporting Information

ABSTRACT: Molecular dynamics calculations and bionformatic studies of dihydrofolate reductase (DHFR) have suggested a network of coupled motions across the whole protein that is correlated to the reaction coordinate. Experimental studies demonstrated that distal residues G121, M42, and F125 in *E. coli* DHFR participate in that network. The missing link in our understanding of DHFR catalysis is the lack of a mechanism by which such remote residues can affect the catalyzed chemistry at the active site. Here, we present a study of the temperature dependence of intrinsic kinetic isotope effects (KIEs) that indicates synergism between a remote residue in that dynamic network, G121, and the active site's residue I14. The intrinsic KIEs for the I14A−G121V double mutant showed steeper temperature dependence ($\Delta E_{a(T\text{-}H)}$) than expected from comparison of the wild type and two single mutants. That effect was nonadditive (i.e., $\Delta E_{a(T\text{-}H)\ G121V} + \Delta E_{a(T\text{-}H)\ I14A} < \Delta E_{a(T\text{-}H)\ \text{double mutant}}$), which indicates a synergism between the two residues. This finding links the remote residues in the network under investigation to the enzyme's active site, providing a mechanism by which these residues can be coupled to the catalyzed chemistry. This experimental evidence validates calculations proposing that both remote and active site residues constitute a network of coupled promoting motions correlated to the bond activation step (C−H → C hydride transfer in this case). Additionally, the effect of I14A and G121V mutations on single turnover rates was additive rather than synergistic. Although single turnover rate measurements are more readily available and thus more popular than assessing intrinsic KIEs, the current finding demonstrates that these rates, which in DHFR reflect several microscopic rate constants, can fall short of revealing the nature of the C−H bond activation per se.

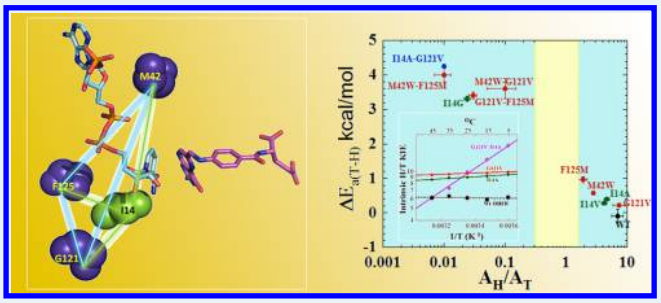

KEYWORDS: *dihydrofolate reductase, kinetic isotope effects, enzyme dynamics, tunneling, dynamic network*

Dihydrofolate reductase (DHFR) is a small (18 kDa) enzyme that catalyzes the reduction of 7,8-dihydrofolate (H_2F) to 5,6,7,8-tetrahydrofolate (H_4F) through a stereospecific transfer of the pro-R hydride from the cofactor, NADPH, to the *si*-face of C_6 of the dihydropterin ring of H_2F. The enzyme is important in maintaining intracellular pools of H_4F, which are used in the biosynthesis of purine nucleotides and some amino acids. Because DHFR plays a vital role in variety of anabolic pathways, it is a common target for antiproliferative therapeutics and has been the subject of many experimental and theoretical studies.[1−11] In particular, the enzyme has emerged as a model for studying the role of dynamics in enzymatic reactions.[8,12−18]

There are several kinds of motions in an enzyme that may affect catalysis. These range from local motions at the active site to long-range motions that span the protein and occur on time scales ranging from seconds to femtoseconds.[13] The term "dynamics" is used here as a broad and comprehensive term covering motions at thermal equilibrium with their environment, which occur on various time scales. These motions include large-scale conformational fluctuations of the protein that occur on a millisecond-to-second time scale, creating a favorable environment for formation of the reactive complexes for the chemical step; the nano- to pico-second fast reorganization of the reaction coordinate, which aids in its reaching the tunneling-ready state (TRS) for efficient H tunneling; and the fast motions directly associated with the reaction coordinate, occurring on a time scale of femto- to picoseconds.[8,11,13,15,17,19−21] Another type of long-range networks of hydrogen bonds that plays a role in modulating the activity of interfacially activated enzymes was discussed by Tawfik and colleagues.[22] This study showed that membrane binding immobilizes long-range interactions via second and third shell residues that reduce the active site's flexibility and preorganizes the catalytic residues.

A common technique used in studying enzyme-catalyzed hydride transfer and the associated dynamics is the measurement of the temperature dependence of kinetic isotope effects (KIEs), studies of which have been carried out for DHFR and several of its mutants.[4,19,23−27] The main advantage of this method, when conducted on intrinsic KIEs rather than on their observed values, is that it is highly sensitive to changes in

Received: February 15, 2015
Revised: April 5, 2015
Published: April 8, 2015

DOI: 10.1021/acscatal.5b00331
ACS Catal. 2015, 5, 3067−3073

hydride donor−acceptor distance (DAD), and reveals information regarding the distribution of DADs at the TRS.[13,28] Analysis of the temperature dependence of intrinsic KIEs has motivated the development of several phenomenological models that assist in interpreting the experimental observations.[13,19,20,28,29] According to these models, temperature-independent KIEs are associated with a narrow distribution of DADs, whereas temperature-dependent KIEs indicate a wider DAD distribution with lower fluctuation frequency.[28,30]

Support for the relationship between DHFR dynamics and function has come from several independent studies employing X-ray crystallography, NMR, and kinetics.[23,24,26,31−34] Hybrid quantum mechanical/molecular mechanics/molecular dynamics (QM/MM/MD) simulations have increasingly provided insight into the nature of conformational sampling in the DHFR-catalyzed reaction, predicting a network of coupled motions extending throughout the protein.[7,11,35−37] QM/MM/MD simulations and bioinformatics analysis (denoted as genomic coupling or coevolution)[38,39] have suggested coupled motions in DHFR that correlates with its catalyzed chemistry. Those studies proposed several residues, both in the active site and distal from it, which could be part of such a network, including G121 and M42. Mutants of G121 and M42 were studied by Benkovic and co-workers, who found that these two residues are coupled to each other and have a synergistic effect on single turnover rates.[31] Furthermore, measurements of the temperature dependence of intrinsic KIEs for the mutants revealed that the coupling of these residues facilitates the catalyzed hydride transfer.[26] Using the same methodology, we recently identified a third distal residue, F125, that is part of the same network.[23] The temperature dependence of the intrinsic KIEs for F125M (8 Å from the active site) indicated that the mutation disrupts the ability of the enzyme to reorganize the TRS, and the much steeper temperature dependence of the intrinsic KIEs of its double mutants with G121V and M42W (i.e., G121V−F125M and M42W−F125M) relative to all single mutants indicated that it is a part of the same network.

In addition to the distal residues, an active site residue, I14, has been predicted to be part of the dynamic network.[36,39,40] NMR studies indicated that this residue exists as two rotamers; only the *trans* rotamer, not seen in either closed or occluded crystal structures, is significantly populated in solution.[41] Modeling studies indicated that in the *trans* rotameric state the side chain of I14 clashes with the nicotinamide ring, forcing it toward the pterine ring. Mutation of I14 to V, A, or G resulted in a progressive increase in the temperature dependence of the intrinsic KIEs as the size of the residue at position 14 was reduced.[25] This was interpreted as resulting from longer and more broadly distributed DADs at the TRS of the mutants with smaller side-chains, which in contrast to the WT no longer restricted the nicotinamide (the H-donnor) fluctuations away from the folate (the H-acceptor). That observation implicated I14 in maintaining optimal positioning of the substrate and cofactor of DHFR for efficient hydride tunneling.[25,28] Figure 1 highlights the position of I14 along with the distal residues that were so far identified experimentally to compose the global network in DHFR.

The missing link in the studies described above is how the distal residues are connected to the active site. Following predictions of QM/MM MD calculations,[7,11,35−37] we searched for synergism between the effect on DAD of an active site residue and a remote residue. The current study examines the relationship between the well-studied distal mutant, G121V,[31,33,35,42−44] and the active-site mutant, I14A. In this work, we measure and analyze the temperature dependence of intrinsic KIEs, and we expand the network of coupled motions to the active site by comparing the effect of a local and remote mutants and their double mutant (I14A, G121V, and I14A−G121V) on the DAD. The results presented below suggest that the remote residue G121 is coupled to the active site residue I14, and that both affect the hydride transfer in a synergistic fashion. This finding provides a mechanism for the coupling of distal residues to the catalyzed chemistry at the active site.

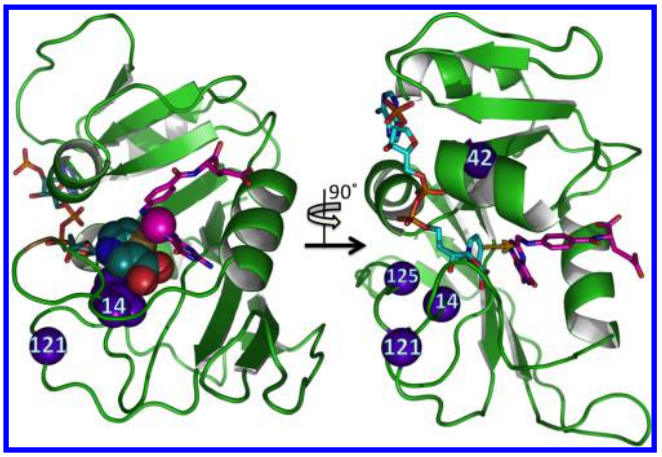

Figure 1. Structure of WT-DHFR (PDB Code 1RX2), with folate in magenta and $NADP^+$ in cyan. *Left panel:* A view demonstrating the location of I14 (purple sphere) as the back support of the H-donor (the nicotinamide ring as spheres, with C4 in gold), keeping it in close contact with the H-acceptor (C6 of the folate, magenta sphere). The remote G121 is also marked and highlighted as a purple sphere. *Right panel:* A view at 90° rotation relative to the left panel, emphasizing the network under study. A gold arrow marks the hydride's path from C4 of the nicotinamide to C6 of the folate, and the α-carbons of residues participating in the network are marked as purple spheres.

EXPERIMENTAL PROCEDURES

Chemicals. All chemicals were reagent grade and used as purchased from Sigma-Aldrich (St. Louis, MO) unless otherwise indicated. [Ad-^{14}C]-NAD^+ and ^{3}H-glucose were purchased from PerkinElmer. [Ad-^{14}C]-NADPH, 4R-[Ad-^{14}C, 4-^{2}H]-NADPH, 4R-^{3}H-NADPH, and 7,8-dihydrofolate were synthesized and stored as per previously published protocols.[45−50] Glucose dehydrogenase from *Bacillus megaterium* (GluDH) was purchased from Affymetrix/USB.

Methods. The I14A−G121V DHFR mutant was constructed using the Stratagene QuikChange site-directed mutagenesis kit and the I14A DHFR plasmid[51] as a template. The forward and reverse primer sequences were 5′-GGAAACGAAACCCTCATCCAAATA-AAGAGTGACGTAAATC-3′ and 5′-GATTTACGTCA-CTCTTTATTTGGATGAGGGTTTCGTTTCC-3′, respectively. Protein expression and purification was carried using previously described protocols.[25,52]

All the kinetic experiments,[9,23,25,26,53] synthesis of labeled cofactors, and data processing were done as described before.[46−49] In brief, to measure the H/T KIEs, NADPH labeled with either H or T at the 4R position were mixed with H_2F and the reaction was initiated with I14A−G121V DHFR at pH 9.0 and the desired temperature. It is important to note that the intrinsic KIEs and the timing of the proton and hydride

DOI: 10.1021/acscatal.5b00331
ACS Catal. 2015, 5, 3067−3073

transfers for the DHFR reactions have previously been shown to be pH-independent.[54] For unlabeled NADPH at position 4, a remote carbon at the adenosine ring was labeled by ^{14}C to serve as a tracer for the conversion of these molecules to product ($NADP^+$). The reaction was quenched at different time points, and the depletion of tritium in the product was monitored as a function of fraction conversion to yield the KIE on the second order rate constant k_{cat}/K_M. D/T KIEs were measured similarly, but with D- instead of H-labeled NADPH at the 4R position. The observed H/T and D/T KIEs were used to calculate the intrinsic KIEs (e.g., k_l/k_h) where l and h represent the light and heavy isotope, respectively. The isotope effect on the activation parameters for the intrinsic KIEs was calculated by nonlinear fit to the Arrhenius equation for intrinsic KIEs:

$$\mathrm{KIE} = \frac{k_l}{k_h} = \frac{A_l}{A_h}\exp\left(\frac{-\Delta E_a}{RT}\right) \quad (1)$$

The single turnover rate of I14A−G121V was measured by monitoring NADPH fluorescence at 450 nm with an Applied Photophysics SX20 stopped-flow spectrophotometer as described previously.[9] In short, 20 μM enzyme was incubated for 5 min with 15 μM NADPH at 25 °C. The solution was then rapidly mixed with 100 μM H_2F and the decay in Förster resonance energy transfer (FRET) was monitored at 450 nm (NADPH emission) upon excitation of the protein at 290 nm. All experiments were carried out in 50 mM MTEN buffer at pH 7.0. Data were fit to a single exponential decay and are reported as the average of five independent measurements with their standard deviation.

RESULTS AND DISCUSSION

Temperature Dependence of the Intrinsic KIEs of I14A−G121V. Primary H/T and D/T KIEs were measured on the second order rate constant, k_{cat}/K_M, between 5 and 45 °C, and intrinsic KIE values were calculated as described before[23,25,26] using the modified Northrop equation (where T, D, and H refer to tritium, deuterium, and protium isotopologues, respectively). The intrinsic KIEs for I14A−G121V DHFR were compared with those from WT,[55] I14A,[51] and G121V.[42] The intrinsic H/T KIEs were fit to the Arrhenius equation for KIEs to obtain the isotope effect on the Arrhenius pre-exponential factor (A_H/A_T) and the activation energy ($\Delta E_{a(T\text{-}H)}$). Figure 2 shows the Arrhenius plot of the intrinsic KIEs for the double mutant, both single mutants, and the WT. Table 1 summarizes the results obtained from fitting the KIEs to the Arrhenius equation.

The temperature (in)dependence of KIEs has stimulated the development of various phenomenological models explaining the experimental observations. These models are denoted as "Marcus-like models", "environmentally coupled tunneling", "tunneling promoting vibrations", "protein promoting vibrations", and more, and have been used to explain C−H bond activations in many enzymes.[13,19,20,26,28,56−58] According to those models, the temperature-independent KIEs observed for a majority of WT enzymes,[19,20,57] including DHFR,[55] indicate a system in which the DAD at the TRS has a narrow distribution (i.e., a well-organized reactive state with a well-reorganized DAD for H-tunneling). A shorter average DAD leads to deflated KIEs, and a broader DAD distribution leads to more temperature-dependent KIEs (i.e., elevated ΔE_a).[13,56]

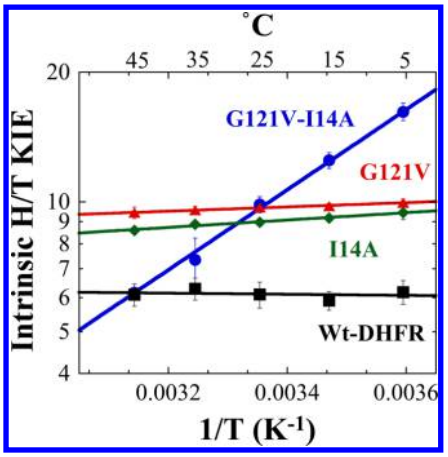

Figure 2. Comparison of Arrhenius plots of intrinsic primary H/T KIEs for WT, G121V, I14A, and G121V−I14A DHFR. The lines represent the nonlinear regression to the Arrhenius equation, and the error bars represent standard deviation.

Comparison of the intrinsic KIEs of I14A−G121V with the corresponding single mutants indicates that the two residues function synergistically to facilitate the hydride transfer reaction catalyzed by the enzyme. The intrinsic KIEs for I14A−G121V showed steep temperature dependence (Figure 2 and Table 1) as compared to the WT and single mutants. The single mutants G121V and I14A have significantly lower temperature-dependent intrinsic KIEs than the corresponding double mutant, and the WT is temperature independent. Accordingly, the average DAD is longer in the single mutants (G121V and I14A) than in the WT; this is revealed by the larger intrinsic KIEs. The slight temperature dependence that is observed for both single mutants indicates that their DAD ensemble is a little broader than it is in the WT. The double mutant, I14A−G121V on the other hand, has a very steep temperature dependence, which indicates that it has much broader distribution of DADs and a poorly reorganized TRS.

It is interesting to note that at room temperature the KIEs for all the three mutants are of similar magnitude, despite the substantial differences in their temperature dependence. This further emphasizes the need to conduct KIE measurements at different temperatures, as measurements only at 25 °C would have led to the erroneous conclusion that the double mutation has the same effect on the hydride transfer reaction as the corresponding single mutants. Furthermore, the temperature dependence of the intrinsic KIEs indicates a significant synergism between G121 and I14. This is evident from the sum of $\Delta E_{a(T\text{-}H)}$ for the single mutants, which is much smaller than $\Delta E_{a(T\text{-}H)}$ for the double mutant ($\Delta E_{a(T\text{-}H)\ G121V} + \Delta E_{a(T\text{-}H)\ I14A} < \Delta E_{a(T\text{-}H)\ \text{double mutant}}$). This nonadditive effect of the double mutant provides for the first time a direct link between a distal residue in the global network of promoting motions in DHFR and the active site of the enzyme.

It is important to note that the single turnover rates (see details below) of I14A−G121V and the corresponding single mutants may initially be taken to suggest that G121 and I14 function independently to facilitate the catalyzed hydride transfer, because the $\Delta\Delta G$ values indicate additive behavior (Table 1). However, as previously discussed and demonstrated,[23,24] single turnover rates do not exclusively represent C−H → C hydride transfer per se, but reflect several microscopic events including protein and ligand conformational

DOI: 10.1021/acscatal.5b00331
ACS Catal. 2015, 5, 3067−3073

Table 1. Comparative Isotope Effects and Single Turnover Rates for WT, G121V, I14A, and I14A−G121V

DHFR	A_H/A_T[a]	$\Delta E_{a(T-H)}$[a] (kcal/mol)	k_{hyd}[b] (s^{-1})	k_{wt}/k_{mut}	$\Delta\Delta G^{\ddagger}$[c] (kcal/mol)
WT[d]	7.0 ± 1.5	−0.1 ± 0.2	228 ± 8		
G121V[e]	7.4 ± 1.6	0.23 ± 0.03	1.4 ± 0.2	163 ± 24	3.01 ± 0.44
I14A[f]	4.7 ± 0.5	0.39 ± 0.06	5.7 ± 0.3	40 ± 2.5	2.18 ± 0.14
I14A−G121V	0.01 ± 0.002	4.25 ± 0.12	0.04 ± 0.001	5700 ± 295	5.11 ± 0.32

[a]Similar trends were observed for H/D and D/T (data not shown). [b]Single turnover rates at 25 °C and pH 7. [c]$\Delta\Delta G^{\ddagger} = RT \ln (k_{wt}/k_{mut})$ at 25 °C. [d]ref 55. [e]ref 42. [f]ref 51.

changes that follow substrate binding (induced fit) and N5−H_2F protonation that occur prior to the hydride transfer step.[54] The kinetic complexity resulting from the multistep step nature of the single turnover measurement necessitates the use of intrinsic KIEs as carried out here to assess possible synergism between multiple residues of DHFR.

Figure 3 presents the isotope effects on Arrhenius parameters for various *E. coli* DHFR mutants and emphasizes the distinct

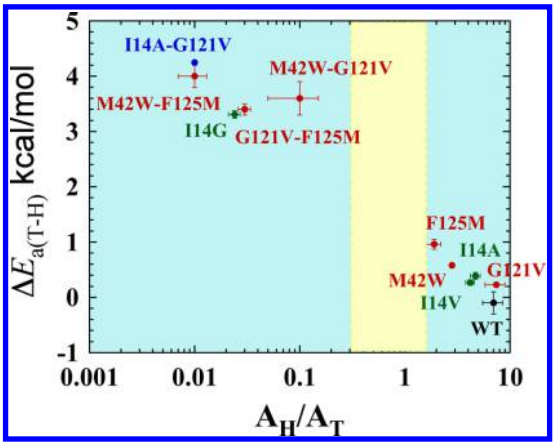

Figure 3. Correlation of Arrhenius parameters (activation energy and pre-exponential factor) of WT (black), distal (red), and local (green) mutants of DHFR. The yellow block represents the semiclassical range of the Arrhenius pre-exponential factor (0.3−1.7). This figure is reproduced from ref with the addition of the double mutant that critically connects the local and distal groups, I14A−G121V (blue).

behavior of the double mutants and I14G from the WT and single mutants. It compares the isotope effect on these parameters for several remote (red) and active site (green) mutants. With the exception of I14G, for which the side chain of the active site residue was dramatically reduced, each single mutation studied gave rise to KIEs that are only slightly temperature dependent. The KIEs for the double mutants, on the other hand, are steeply temperature-dependent, with $\Delta E_{a(T-H)}$ values that are nonadditive when compared with the corresponding single mutations. As described previously,[23] this strongly suggests that the residues act synergistically to facilitate the catalyzed hydride transfer reaction. Importantly, the results presented here for the I14A−G121V double mutant (blue point in Figure 3) strongly indicates a similar synergistic behavior and connects a distal residue (G121) to the active site of the enzyme (via I14). Such a connection between long-range and active site protein motions delineates a mechanism by which the global network of coupled motions in DHFR functions to catalyze hydride transfer.

Quantitative Analysis of DAD Fluctuations from the Temperature Dependence of Intrinsic KIEs. In order to assess the average DAD and its distribution from the size and temperature dependence of KIEs, we fit the intrinsic KIEs to a phenomenological model, yielding parameters more directly relevant to the DAD and its distribution than are the isotope effects on entropy and enthalpy yielded by the Arrhenius analysis.[28] KIEs with no or moderate temperature dependence ($\Delta E_{a(T-H)} < 1$ kcal/mol) can be fit to a single-population model, which results in two parameters: DAD_0 (average DAD), and f (a force constant identifying the potential energy surface for the DAD's fluctuations—larger values of f correspond to narrower DAD distributions). However, for KIEs with a steep temperature dependence ($\Delta E_{a(T-H)} > 1$ kcal/mol), the data can only be fit to a two-populations model, where tunneling occurs in the predominant population and hydride transfer occurs over the reaction barrier in the other population. The latter model also gives two parameters: DAD_{long} (average DAD of the population with longer DADs) and $\Delta G°$ (difference in free energy between the two populations).[28] Because the latter model can fit any temperature-dependent KIEs, it is often useful in the comparison of different isozymes, where a shorter DAD_{long} indicates shorter average DAD. The relations between the parameter $\Delta G°$ and the distribution of DADs have a more complex trend, which is indicated by the yellow arrow in Figure 4.

As is apparent from Tables 1 and 2, WT DHFR exhibits temperature-independent KIEs, indicating a narrow distribution of DAD for hydride transfer and a well-organized TRS. The single mutants G121V (**a** in Figure 4) and I14A (**b** in Figure 4) both exhibit some temperature dependence in the intrinsic KIEs ($0 < \Delta E_a < 1$ kcal/mol), as do several other single

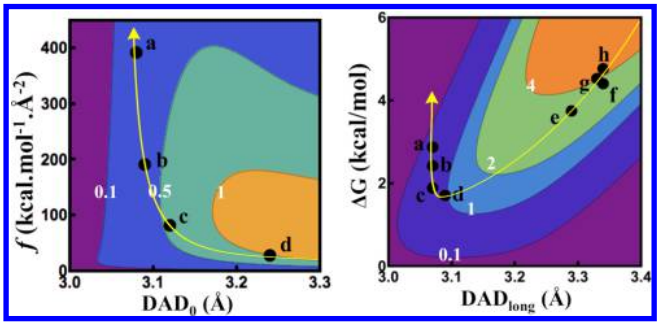

Figure 4. Contour plots of ΔE_a between E_a for tritium and E_a for hydrogen in kcal/mol (values in white digits) as a function of *Left*: average DAD (DAD_0) and force constant (f), and *Right*: DAD of the major population, i.e., lower energy and longer average DAD (DAD_{long}) and the difference in free energy between the two populations ($\Delta G°$). The black dots represent the different mutants and are labeled as follows: a, G121V; b, I14A; c, M42W; d, F125M; e, G121V−F125M; f, M42W-G121V; g, M42W−F125M; h, I14A−G121V. Since the errors are too large for WT, it is not shown in the figure. The errors for other points are smaller than the dot representing the data. The yellow arrow points toward better-organized TRS.

DOI: 10.1021/acscatal.5b00331
ACS Catal. 2015, 5, 3067−3073

Table 2. Regression Parameters of Intrinsic KIEs to a Marcus-Like Model

	1 population		2 populations	
DHFR	DAD_0[a] (Å)	f (kcal/mol/ Å ^{2})	DAD_L[a] (Å)	$\Delta G°$ (kcal/mol)
WT[c]	3.06	NA[b]	3.06	NA[b]
G121V[c]	3.08	390	3.07	2.86
I14A[c]	3.09	190	3.07	2.40
I14A−G121V			3.34	4.75

[a]Errors are <5% of the reported value. [b]Not applicable because for the WT, where the KIEs are temperature independent within experimental errors ($\Delta E_a \sim 0$), the experimental value is smaller than its error; the errors for the other systems are <15% of the reported value. [c]ref28.

mutants (Figure 4, left panel). The I14A−G121V double mutant (**h** in Figure 4) has much steeper temperature dependence in its KIE and could not be fitted using a one-population model. Consequently only the two-population model was used to fit the data and to compare all the mutants (the right panels of Table 2 and Figure 4). The distal-active-site double mutant (I14A−G121V) has similar parameters ($\Delta G°$ and DAD_{long}) to those of the previously studied distal−distal double mutants (M42W−G121V, G121V−F125M and M42W−F125M).[23] The new double mutant reported here reveals a missing link between remote residues (G121, M42, and F125) and the active site residue (I14) that is directly associated with the formation of a well-organized TRS for the catalyzed hydride transfer step.[25]

Single Turnover Rates. The single turnover rate of I14A−G121V DHFR was measured under the same conditions as the WT and two single mutants (pH 7.0 and 25 °C), and the results are presented in Table 1. The I14A−G121V double mutant had a dramatically lower single turnover rate than did the WT and single mutants, but that reduction in rate was additive in nature ($\Delta G^{‡}_{G121V} + \Delta G^{‡}_{I14A} = \Delta G^{‡}_{double\ mutant}$), failing to indicate that residues G121 and I14 are coupled to each other. However, as described above and in refs 23,24, the single turnover rate is not a measure of the C−H → C hydride transfer step per se because it includes several microscopic rate constants. At a minimum, these include ligands and protein rearrangements that follow substrate binding, protonation of the N5 of H_2F, and the subsequent hydride transfer step. The additive nature of the single turnover rates (Table 1, right column) indicates that the millisecond-scale events *prior to the C−H bond activation* do not involve coupling between residues G121 and I14. The synergy observed for the intrinsic KIEs on the C−H → C hydride transfer step, on the other hand, indicates a coupling between these local and distal residues directly affecting the chemical conversion at the active site.

Kinetic Complexity. A feature frequently observed in enzymatic systems is that isotopically insensitive kinetic steps (substrate binding or release, conformational changes, product release, etc.) mask the intrinsic KIEs. This is referred to as kinetic complexity and results in observed KIEs that are smaller than their intrinsic KIEs, as described by eq 2:[59]

$$KIE_{obs} = \frac{KIE_{int} + C_f}{1 + C_f} \quad (2)$$

where KIE_{obs} is the observed KIE, KIE_{int} is the intrinsic KIE, and C_f is the forward commitment to catalysis, which is the ratio between the rate of the forward, isotopically sensitive step, and the rates of the preceding, backward, isotopically insensitive steps.[59] The Arrhenius plots of the commitment to catalysis on the second-order rate constant k_{cat}/K_M for WT DHFR and its mutants are presented in Figure 5. It is apparent from Figure 5

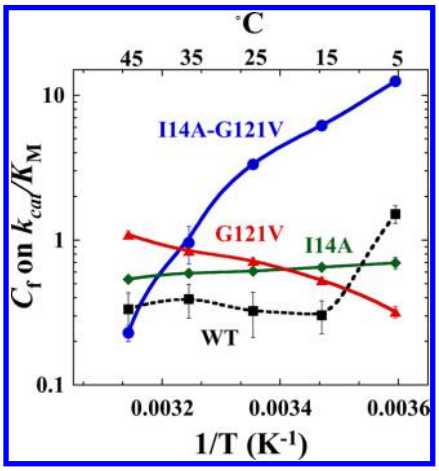

Figure 5. Arrhenius plots of commitments (C_f) on k_{cat}/K_M for hydride transfer for WT[55] (black), I14A[51] (green), G121V[42] (red), and I14A−G121V (blue). The C_f values are presented as average values with standard deviations as calculated from eq 2. The lines are an interpolation of the data and do not represent an analytical fitting.

that the double mutant has a C_f very different than that of either the single mutants or the WTs. As is true of the WT and single mutants, the nonlinear temperature dependence of the double mutant's C_f indicates that the kinetic complexity arises not from a single step but from multiple kinetic steps occurring before the first irreversible step during catalytic turnover. The nonlinear Arrhenius plots for C_f indicate that the kinetic complexity does not reflect a single step, thus it is not possible rigorously compare the effects of the different mutants on that parameter.

CONCLUSIONS

One of the most pressing questions in contemporary enzymology is the role of protein motions in catalysis. Here we used DHFR from *E. coli* and its catalyzed reaction (C−H → C hydride transfer) as a model system to examine this question. Previous QM/MM/MD calculations identified several residues remote form the active site, including G121, F125, and M42, as part of a dynamic network of coupled motions associated with the hydride transfer step in DHFR.[7,35,39] Measurements of the temperature dependence of the intrinsic KIEs of these distal mutants confirmed that these residues are coupled to each other and correlated to the hydride transfer reaction.[23,26]

The main missing link at this point was the understanding of how residues remote from the active site alter the direct environment of the H donor and acceptor, their average DAD at the TRS, and the distribution of the DAD. Here we tested the prediction of computer simulations,[36,39,40] suggesting that active site residue I14 could be part of the same network of dynamic motions coupled to the chemical step. Recently, I14

DOI: 10.1021/acscatal.5b00331
ACS Catal. 2015, 5, 3067−3073

has been used as a benchmark to relate the temperature dependence of intrinsic KIEs to the distribution of DAD and its fluctuations.[25] We used the same kinetic tools used in the past to identify coupling between one of the remote residues, G121, the active site residue, I14, and the chemical step.

A synergistic effect of these residues is evident from the quantitative comparison of the temperature dependence of the two single mutants (I14A and G121V) and their double mutant ($\Delta E_{a\ G121V} + \Delta E_{a\ I14A} < \Delta E_{a\ double\ mutant}$, see Table 1). The comparison of single turnover rates indicated that each mutant affects this rate, but the effect was additive ($\Delta\Delta G^{\ddagger}_{G121V} + \Delta\Delta G^{\ddagger}_{I14A} = \Delta\Delta G^{\ddagger}_{double\ mutant}$, see Table 1), indicating no effect of the residues coupling on this rate, which includes several microscopic rates as discussed above. The kinetic complexity on k_{cat}/K_M (C_f) confirmed that steps prior to hydride transfer are affected by the single mutations, and more so by the double mutation, but this factor is hard to quantify and thus cannot reveal synergism between the remote and active site residues. This is an example where the single turnover rates failed to examine the nature of the bond activation step, whereas intrinsic KIEs reflecting effects on the C−H → C hydride transfer per se, revealed synergism between the two residues under study. A complementary explanation for the different trends in k_{hyd} and the intrinsic KIEs is that the heavy isotope (examined only in the KIEs study) is much more sensitive to changes in the reaction's TS (or TRS) than the light protium transfer (reflected by k_{hyd}). Indeed, that heavier isotope is much more localized than the light protium, and thus, its transfer across a barrier would be more sensitive to any alteration of the reaction's barrier or the DAD.

The findings indicate that an active site residue (I14) that has a direct effect on the distance and dynamics of the DAD for the C−H → C hydride transfer step catalyzed by DHFR is also part of the dynamic network of functional motions involving remote residues such as G121, M42, and F125. The findings demonstrate a mechanism for remote residues to be coupled to the chemistry in active site. This path has not been examined experimentally before and its identification greatly improves our understanding of DHFR catalysis in ways that static X-ray structures alone cannot. This finding promotes the notion that biological macromolecules evolved to act holistically, where dynamics of residues across the molecule are coupled to each other in conducting its function (catalysis of C−H bond activation in this case).

■ ASSOCIATED CONTENT

Supporting Information

The following file is available free of charge on the ACS Publications website at DOI: 10.1021/acscatal.5b00331.

Arrhenius plot for observed (H/T and D/T) and intrinsic (H/T, H/D, and D/T) KIE and observed and intrinsic KIE values for I14A−G121V are provided (PDF)

■ AUTHOR INFORMATION

Corresponding Author

*E-mail: amnon-kohen@uiowa.edu. Tel.: +1 319 335 0234.

Notes

The authors declare no competing financial interest.

■ ACKNOWLEDGMENTS

This work was supported by NIH (R01GM65368) and NSF (CHE-1149023).

■ REFERENCES

(1) Adamczyk, A. J.; Cao, J.; Kamerlin, S. C. L.; Warshel, A. *Proc. Natl. Acad. Sci. U. S. A.* **2011**, *108*, 14115−14120.
(2) Hammes, G. G.; Benkovic, S. J.; Hammes-Schiffer, S. *Biochemistry* **2011**, *50*, 10422−10430.
(3) Liu, H.; Warshel, A. In *Quantum Tunnelling in Enzyme-Catalysed Reactions*; Allemann, R. K., Scrutton, N. S., Eds.; The Royal Society of Chemistry: Cambridge, U.K., 2009; pp 242−267.
(4) Ruiz-Pernia, J. J.; Luk, L. Y. P.; García-Meseguer, R.; Martí, S.; Loveridge, E. J.; Tuñón, I.; Moliner, V.; Allemann, R. K. *J. Am. Chem. Soc.* **2013**, *135*, 18689−18696.
(5) Fan, Y.; Cembran, A.; Ma, S.; Gao, J. *Biochemistry* **2013**, *52*, 2036−2049.
(6) Sawaya, M. R.; Kraut, J. *Biochemistry* **1997**, *36*, 586−603.
(7) Rod, T. H.; Radkiewicz, J. L.; Brooks, C. L. *Proc. Natl. Acad. Sci. U. S. A.* **2003**, *100*, 6980−6985.
(8) Dametto, M.; Antoniou, D.; Schwartz, S. D. *Mol. Phys.* **2012**, *110*, 531−536.
(9) Fierke, C. A.; Johnson, K. A.; Benkovic, S. J. *Biochemistry* **1987**, *26*, 4085−4092.
(10) Grubbs, J.; Rahmanian, S.; DeLuca, A.; Padmashali, C.; Jackson, M.; Duff, M. R.; Howell, E. E. *Biochemistry* **2011**, *50*, 3673−3685.
(11) Radkiewicz, J. L.; Brooks, C. L. *J. Am. Chem. Soc.* **2000**, *122*, 225−231.
(12) Hammes-Schiffer, S. *Acc. Chem. Res.* **2005**, *39*, 93−100.
(13) Klinman, J. P.; Kohen, A. *Annu. Rev. Biochem.* **2013**, *82*, 471−496.
(14) Francis, K.; Kohen, A. *Curr. Opin. Chem. Biol.* **2014**, *21*, 19−24.
(15) Glowacki, D. R.; Harvey, J. N.; Mulholland, A. J. *Nat. Chem.* **2012**, *4*, 169−176.
(16) Lee, J.; Goodey, N. M. *Chem. Rev.* **2011**, *111*, 7595−7624.
(17) Liu, H.; Warshel, A. *J. Phys. Chem. B* **2007**, *111*, 7852−7861.
(18) Kamerlin, S. C. L.; Warshel, A. *Proteins: Struct., Funct., Genet.* **2010**, *78*, 1339−1375.
(19) Nagel, Z. D.; Klinman, J. P. *Chem. Rev.* **2010**, *110*, PR41−PR67.
(20) Hay, S.; Scrutton, N. S. *Nat. Chem.* **2012**, *4*, 161−168.
(21) Kohen, A. In *Isotopes Effects in Chemistry and Biology*; Kohen, A., Limbach, H.-H., Eds.; Taylor and Francis: Boca Raton, FL, 2006; pp 743−764.
(22) Ben-David, M.; Sussman, J. L.; Maxwell, C. I.; Szeler, K.; Kamerlin, S. C. L.; Tawfik, D. S. *J. Mol. Biol.* **2015**, *427*, 1359−1374.
(23) Singh, P.; Sen, A.; Francis, K.; Kohen, A. *J. Am. Chem. Soc.* **2014**, *136*, 2575−2582.
(24) Francis, K.; Stojković, V.; Kohen, A. *J. Biol. Chem.* **2013**, *288*, 35961−35968.
(25) Stojković, V.; Perissinotti, L. L.; Willmer, D.; Benkovic, S. J.; Kohen, A. *J. Am. Chem. Soc.* **2012**, *134*, 1738−1745.
(26) Wang, L.; Goodey, N. M.; Benkovic, S. J.; Kohen, A. *Proc. Natl. Acad. Sci. U. S. A.* **2006**, *103*, 15753−15758.
(27) Maglia, G.; Allemann, R. K. *J. Am. Chem. Soc.* **2003**, *125*, 13372−13373.
(28) Roston, D.; Cheatum, C. M.; Kohen, A. *Biochemistry* **2012**, *51*, 6860−6870.
(29) Kohen, A. *Acc. Chem. Res.* **2015**, *48*, 466−473.
(30) Roston, D.; Islam, Z.; Kohen, A. *Molecules* **2013**, *18*, 5543−5567.
(31) Rajagopalan, P. T. R.; Stefan, L.; Benkovic, S. J. *Biochemistry* **2002**, *41*, 12618−12628.
(32) Boehr, D. D.; McElheny, D.; Dyson, H. J.; Wright, P. E. *Proc. Natl. Acad. Sci. U. S. A.* **2010**, *107*, 1373−1378.
(33) Antikainen, N. M.; Smiley, R. D.; Benkovic, S. J.; Hammes, G. G. *Biochemistry* **2005**, *44*, 16835−16843.
(34) Boehr, D. D.; McElheny, D.; Dyson, H. J.; Wright, P. E. *Science* **2006**, *313*, 1638−1642.

DOI: 10.1021/acscatal.5b00331
ACS Catal. 2015, 5, 3067−3073

(35) Wong, K. F.; Selzer, T.; Benkovic, S. J.; Hammes-Schiffer, S. *Proc. Natl. Acad. Sci. U. S. A.* **2005**, *102*, 6807−6812.
(36) Agarwal, P. K.; Billeter, S. R.; Rajagopalan, P. T.; Benkovic, S. J.; Hammes-Schiffer, S. *Proc. Natl. Acad. Sci. U. S. A.* **2002**, *99*, 2794−2799.
(37) Roston, D.; Kohen, A.; Doron, D.; Major, D. T. *J. Comput. Chem.* **2014**, *35*, 1411−1417.
(38) Ramanathan, A.; Agarwal, P. K. *PLoS Biol.* **2011**, *9*, e1001193.
(39) Hammes-Schiffer, S.; Benkovic, S. J. *Annu. Rev. Biochem.* **2006**, *75*, 519−541.
(40) Agarwal, P. K.; Billeter, S. R.; Hammes-Schiffer, S. *J. Phys. Chem. B* **2002**, *106*, 3283−3293.
(41) Schnell, J. R.; Dyson, H. J.; Wright, P. E. *Biochemistry* **2003**, *43*, 374−383.
(42) Wang, L.; Tharp, S.; Selzer, T.; Benkovic, S. J.; Kohen, A. *Biochemistry* **2006**, *45*, 1383−1392.
(43) Boehr, D. D.; Schnell, J. R.; McElheny, D.; Bae, S.-H.; Duggan, B. M.; Benkovic, S. J.; Dyson, H. J.; Wright, P. E. *Biochemistry* **2013**, *52*, 4605−4619.
(44) Mauldin, R. V.; Sapienza, P. J.; Petit, C. M.; Lee, A. L. *PLoS One* **2012**, *7*, e33252.
(45) Agrawal, N.; Kohen, A. *Anal. Biochem.* **2003**, *322*, 179−184.
(46) Markham, K. A.; Sikorski, R. S.; Kohen, A. *Anal. Biochem.* **2004**, *322*, 26−32.
(47) Markham, K. A.; Sikorski, R. S.; Kohen, A. *Anal. Biochem.* **2004**, *325*, 62−67.
(48) McCracken, J. A.; Wang, L.; Kohen, A. *Anal. Biochem.* **2003**, *324*, 131−136.
(49) Sen, A.; Yahashiri, A.; Kohen, A. *Biochemistry* **2011**, *50*, 6462−6468.
(50) Blakley, R. L. *Nature* **1960**, *188*, 231−232.
(51) Stojković, V.; Perissinotti, L. L.; Lee, J.; Benkovic, S. J.; Kohen, A. *Chem. Commun.* **2010**, *46*, 8974−8976.
(52) Cameron, C. E.; Benkovic, S. J. *Biochemistry* **1997**, *36*, 15792−15800.
(53) Wang, Z.; Singh, P.; Czekster, C. M.; Kohen, A.; Schramm, V. L. *J. Am. Chem. Soc.* **2014**, *136*, 8333−8341.
(54) Liu, C. T.; Francis, K.; Layfield, J. P.; Huang, X.; Hammes-Schiffer, S.; Kohen, A.; Benkovic, S. J. *Proc. Natl. Acad. Sci. U. S. A.* **2014**, *111*, 18231−18236.
(55) Sikorski, R. S.; Wang, L.; Markham, K. A.; Rajagopalan, P. T.; Benkovic, S. J.; Kohen, A. *J. Am. Chem. Soc.* **2004**, *126*, 4778−4779.
(56) Cheatum, C.; Kohen, A. In *Dynamics in Enzyme Catalysis*; Klinman, J., Hammes-Schiffer, S., Eds.; Springer Berlin Heidelberg: Berlin Heidelberg, 2013; Vol. *337*, pp 1−39.
(57) Kanaan, N.; Ferrer, S.; Martí, S.; Garcia-Viloca, M.; Kohen, A.; Moliner, V. *J. Am. Chem. Soc.* **2011**, *133*, 6692−6702.
(58) Wang, Z.; Abeysinghe, T.; Finer-Moore, J. S.; Stroud, R. M.; Kohen, A. *J. Am. Chem. Soc.* **2012**, *134*, 17722−17730.
(59) Cook, P. F.; Cleland, W. W.; Taylor and Francis Group LLC: New York, NY, 2007; pp 253−324.

DOI: 10.1021/acscatal.5b00331
ACS Catal. 2015, 5, 3067−3073